Prediction of Flood/Debris Flow Hydrograph Due to Landslide Dam Failure by Overtopping and Sliding

Ripendra AWAL*, Hajime NAKAGAWA, Kenji KAWAIKE, Yasuyuki BABA and Hao ZHANG

* Graduate School of Engineering, Kyoto University

Synopsis

An integrated model was developed by combining three separate models: (i) model of seepage flow, (ii) model of slope stability and (iii) model of dam surface erosion and flow to predict flood/debris flow hydrograph resulted from failure of landslide dam by overtopping and sudden sliding. The main advantage of an integrated model is that it can detect failure mode due to either overtopping or sliding based on initial and boundary conditions. The proposed model is tested for three different experimental cases of landslide dam failure due to overtopping and sliding, and reasonably reproduced the resulting flood/Debris flow hydrograph.

Keywords: landslide dam, slope stability, seepage flow, overtopping flow, flood/debris flow hydrograph

1. Introduction

Earthquakes or heavy rainfall and snow melt may cause landslides and debris flow on the slopes in the vicinity of river channel. If the sediment mass generated by such landslides are big enough and reaches the river may sometimes block a river flow and create a landslide dam naturally. Formation and failure of landslide dam are one of the significant natural hazards in the mountainous area all over the world. Landslide dams are also common in Japan because of widespread unstable slopes and narrow valleys exist in conjunction with frequent hydrologic, volcanic and seismic landslide triggering events (Swanson, 1986). Historical documents and topography have revealed the formation of many landslide dams, some of which broke and caused major damage in Japan (Tabata et al., 2002). The 2004 Chuetsu earthquake resulted in many landslide dams particularly in the Imo River basin. In 2005, typhoon 14 caused a large landslide dam near the Mimi-kawa river (Mizuyama, 2006).

The catastrophic failure of landslide dam may occur shortly after its formation. Prediction of potential peak discharge and resulting hydrograph is necessary for the management of dam-break flood hazards and to decide appropriate mitigation measures including evacuation. The predicted outflow hydrograph will serve as an upstream boundary condition for subsequent flood routing to predict inundation area and hazard in the downstream. Sudden, rapid and uncontrolled release of water impounded in landslide dam has been responsible for some major disasters in mountainous region. Peak discharge produced by such events may be many times greater than the mean annual maximum instantaneous flood discharge.

Basically, there are two methods to predict probable peak discharge from potential failure of landslide dam (Walder and O'Connor, 1997). One method relies on regression equations that relate
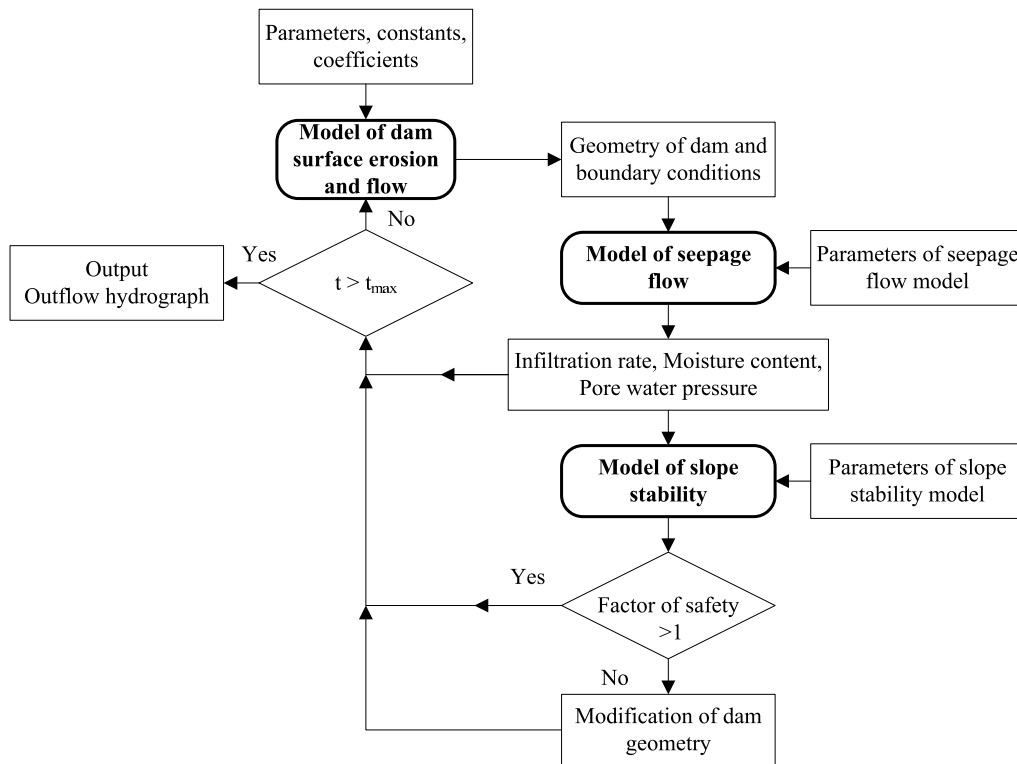
Fig. 1 General flow chart of an integrated model to predict flood/debris flow hydrograph due to landslide dam failure.

observed peak discharge of landslide dam failure to some measure of impounded water volume: depth, volume, or some combination thereof (Costa, 1985, Costa and Schuster 1988, Walder and O'Connor, 1997) and regression equations that relate experimental peak discharge to some measure of impounded water volume: depth, torrent bed gradient and inflow discharge (Tabat et al., 2001). The other method employs computer implementation of a physically based mathematical model. Several researchers have developed physically based model such as Fread (1991), Takahashi and Kuang (1988), Takahashi and Nakagawa (1994), Mizuyama (2006) and Satofuka et al. (2007). Although, landslide dam failure is frequently studied as an earthen dam failure, very few models are developed for landslide dam failure that can treat the flow as both sediment flow and debris flow. If the concentration of sediment is above 10%, non-newtonian viscous flow has to be taken into account. During surface erosion of landslide dam, sediment concentration increased more than 10%, so the model to predict the flood/debris flow hydrograph due to landslide dam failure should be capable to treat all types of flow

based on sediment concentration.

Most of the existing models are applicable to overtopping failure of landslide dam. Some model has limitation to represent downstream batter slopes of greater than 1 in 5 (Davies, 2007). Infiltration process is neglected in almost all available models. In this context, an attempt has been made to incorporate integration of three separate models: (i) model of seepage flow, (ii) model of slope stability and (iii) model of dam surface erosion and flow to predict the outflow hydrograph resulted from failure of landslide dam by overtopping and sudden sliding. The main advantage of an integrated model is that it can predict time at which landslide dam may fail and also detect failure mode due to either overtopping or sliding based on initial and boundary conditions.

2. Numerical model

The model of the landslide dam failure to predict flood/debris flow hydrograph consists of three models. The seepage flow model calculates pore water pressure and moisture content inside the dam body. The model of slope stability calculates the

factor of safety and the geometry of critical slip surface according to pore water pressure, moisture movement in the dam body and water level in the upstream reservoir. The model of dam surface erosion and flow calculates dam surface erosion due to overflowing water. General outline of proposed integrated model is shown in Fig. 1. A brief description of each model is given below.

2.1 Model of seepage flow

The seepage flow in the dam body is caused by the blocked water stage behind the dam. The transient flow in the dam body after formation of landslide dam can be analyzed by Richards' equation. To evaluate the change in pore water pressure in variably saturated soil, pressure based Richards' equation is used (Awal et al., 2007).

$$C\frac{\partial h}{\partial t} = \frac{\partial}{\partial x}\left(K_x(h)\frac{\partial h}{\partial x}\right) + \frac{\partial}{\partial z}\left(K_z(h)\left(\frac{\partial h}{\partial z}+1\right)\right) \quad (1)$$

where h is the water pressure head, $K_x(h)$ and $K_z(h)$ are the hydraulic conductivity in x and z direction, C is the specific moisture capacity $(\partial\theta/\partial h)$, θ is the soil volumetric water content, t is the time, x is the horizontal spatial coordinate and z is the vertical spatial coordinate taken as positive upwards. Eq.(1) represents flow in both the unsaturated domain as well as in the saturated domain. Line-successive over-relaxation (LSOR) is often a very effective method of treating cross-sectional problem grids. LSOR scheme is used in this study for the numerical solution of Richards' equation.

In order to solve Richards' equation, the constitutive equations, which relate the pressure head to the moisture content and the relative hydraulic conductivity, are required. In this study, constitutive relationships proposed by van Genuchten (1980) are used for establishing relationship of $K-h$ and $\theta-h$, with $m = 1-(1/\eta)$.

2.2 Model of slope stability

The evaluation of transient slope stability of landslide dam by the limit equilibrium method involves calculating the factor of safety and searching for the critical slip surface that has the lowest factor of safety. Many attempts have been conducted to locate the position of critical slip surface by using general noncircular slip surface theory coupled with different non-linear programming methods. The numerical procedure behind the identification of critical noncircular slip surface with the minimum factor of safety based on dynamic programming and the Janbu's simplified method is mainly based on research by Yamagami and Ueta (1986). The algorithm combines the Janbu's simplified method with dynamic programming on the basis of Baker's successful procedure.

Janbu's simplified method can be used to calculate the factor of safety for slip surfaces of any shape. The sliding mass is divided into vertical slices and the static equilibrium conditions of each slice are considered as sum of the vertical forces equal to zero and sum of the forces parallel to failure surface equal to zero. For the soil mass as a whole, sum of the vertical forces $\sum F_y = 0$ and sum of the horizontal forces $\sum F_x = 0$ are considered as equilibrium condition.

Based on the above considerations the factor of safety, F_s for Janbu's simplified method is defined as:

$$F_s = \frac{1}{\displaystyle\sum_{i=1}^{n} W_i \tan\alpha_i} \times$$

$$\sum_{i=1}^{n}\left\{\frac{cl_i\cos\alpha_i + (W_i - u_il_i\cos\alpha_i)\tan\phi}{\cos^2\alpha_i\left(1+\dfrac{1}{F_s}\tan\alpha_i\tan\phi\right)}\right\} \quad (2)$$

where W_i is the weight of each slice including surface water, l_i is the length of the base of each slice, u_i is the average pore water pressure on the base of the slice, α_i is the inclination of the base to the horizontal, n is the total number of slices, and c and ϕ are the Mohr-Coulomb strength parameters.

The details of transient slope stability analysis of landslide dam by using dynamic programming and Janbu's simplified method can be found in Awal et al. (2007).

2.3 Model of dam surface erosion and flow

There are only a few two-dimensional (2D) numerical models for dam-break erosion by overtopping flow. Takahashi and Nakagawa (1994) used 2D model to predict flood/debris flow hydrograph due to natural dam failure caused by overtopping. Broich (1998) used 2D model using different numerical schemes for shallow water equations, Exners equation and sediment transport formulae. Unrealistic modeling of the vertical and lateral erosion, no stability mechanism, and parabolic breach shape are the some limitations of this model (Morris and Hassan, 2002).

The mathematical model developed by Takahashi and Nakagawa (1994) was used for the modeling of surface erosion and flow. The model was capable to analyse the whole phenomena from the beginning of overtopping to the complete failure of the dam as well as to predict flood/debris flow hydrograph in the downstream. The infiltration in the dam body was not considered in their model; therefore, time to overflow after formation of landslide dam could not be predicted from the previous model. In this study, infiltration in the dam body is also incorporated.

The model is two-dimensional and it can also collapse to treat one-dimensional for overtopping from full channel width. In case of sudden sliding failure, simplified assumption is made for initial transformation of the dam body after the slip failure. Based on many experiments the slipped mass is assumed to stop at the sliding surface where slope is less than angle of repose and the shape of the slipped mass is assumed as trapezium. There is some time lag between slip failure and movement of the slipped soil mass but in the model, the time necessary for such a deformation is assumed as nil. The erosion process by the overspilled water is analysed for the modified dam shape.

The erosive action of the overtopping flow removes material from the top part of the dam. The overtopped flow grows to debris flow by adding the eroded dam material to it, if the slope and length of dam body satisfy the critical condition for the occurrence of a debris flow.

The main governing equations are briefly discussed here. The depth-wise averaged two-dimensional momentum conservation equation for the x-wise (down valley) direction is

$$\frac{\partial M}{\partial t} + \beta^{'} \frac{\partial(uM)}{\partial x} + \beta^{'} \frac{\partial(vM)}{\partial y} = gh\sin\theta_{bxo}$$
$$- gh\cos\theta_{bxo} \frac{\partial(h + z_b)}{\partial x} - \frac{\tau_{bx}}{\rho_T} \qquad (3)$$

and for the y-wise (lateral) direction,

$$\frac{\partial N}{\partial t} + \beta^{'} \frac{\partial(uN)}{\partial x} + \beta^{'} \frac{\partial(vN)}{\partial y} = gh\sin\theta_{byo}$$
$$- gh\cos\theta_{byo} \frac{\partial(h + z_b)}{\partial y} - \frac{\tau_{by}}{\rho_T} \qquad (4)$$

The continuity of the total volume is

$$\frac{\partial h}{\partial t} + \frac{\partial M}{\partial x} + \frac{\partial N}{\partial y} = i\{c_* + (1 - c_*)s_b\} - q \qquad (5)$$

The continuity equation of the particle fraction is

$$\frac{\partial(ch)}{\partial t} + \frac{\partial(cM)}{\partial x} + \frac{\partial(cN)}{\partial y} = ic_* \qquad (6)$$

The equation for the change of bed surface elevation is

$$\frac{\partial z_b}{\partial t} + i = i_{sml} + i_{smr} \qquad (7)$$

where $M = uh$ and $N = vh$ are the x and y components of flow flux, u and v are the x and y components of mean velocity, h is the flow depth, z_b is the elevation, ρ_T is the apparent density of the flow, $\rho_T = c(\sigma - \rho) + \rho$, c is the volume concentration of the solids fraction in the flow, σ is the density of the solids, ρ is the density of water, $\beta^{'}$ is the momentum correction coefficient, τ_{bx} and τ_{by} are the x and y components of
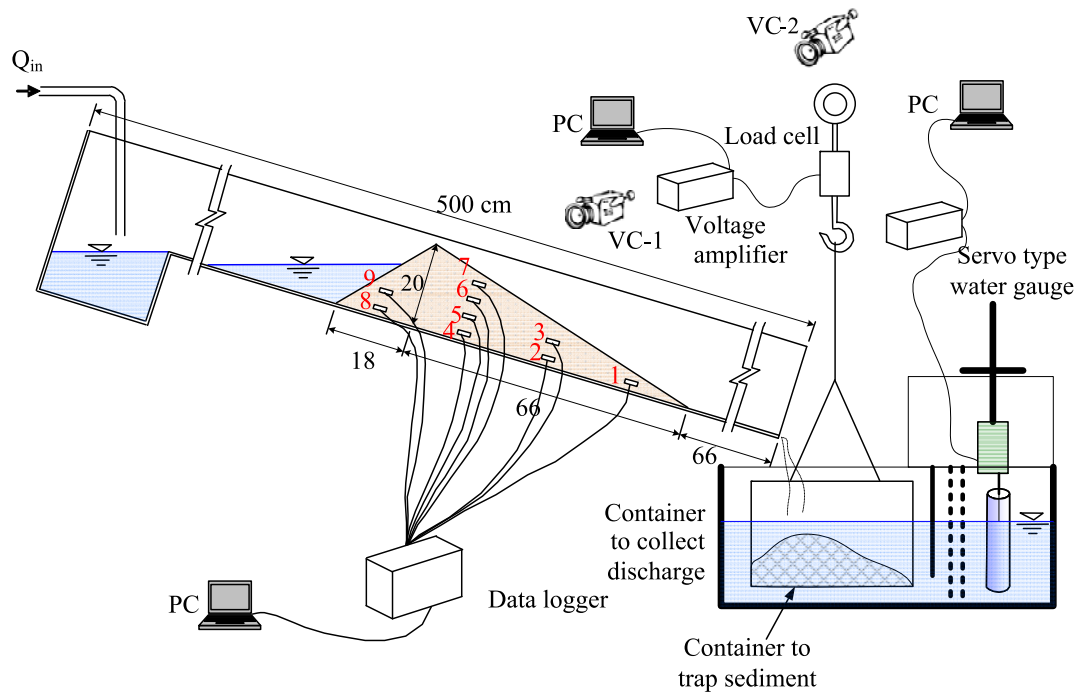
Fig. 2 Experimental setup

resistance to flow, i is the erosion or deposition velocity, c_* is the solids fraction in the bed, s_b is the degree of saturation in the bed (applicable only in cases of erosion, when deposition takes place substitute $s_b = 1$), i_{sml} and i_{smr} are the mean recessing velocity of the left and right hand side banks of the incised channel, respectively, t is the time, g is the acceleration due to gravity and q is the infiltration rate.

Shear stress, erosion or deposition velocity and channel enlargement for overtopping from partial channel width were evaluated using the model presented in Takahashi and Nakagawa (1994).

3. Experimental study

A rectangular flume of length 5m, width 20cm and depth 21cm was used. The slope of the flume was set at 17 degree. Mixed silica sand of mean diameter 1mm was used to prepare a triangular dam in the flume. The height of the dam was 20cm and the longitudinal base length was 84cm. The schematic diagram of the flume is shown in Fig. 2. van Genuchten parameters (including θ_r) were estimated by non-linear regression analysis of soil moisture retention data obtained by pF meter

experiment. Some other parameters of mixed sand are listed in Table 1.

Table 1 Some parameters of the sediment considered

Sediment type	SMix
Saturated moisture content, θ_{sat}	0.287
Residual moisture content, θ_{res}	0.045
α	5.50
η	3.20
Specific gravity, Gs	2.65
Mean grain size, D_{50} (mm)	1.00
Angle of repose, ϕ (degree)	34

4. Results and discussions

The shape of the dam body at different time step due to surface erosion after overtopping and the shape of slip surface during sliding were measured by analyses of video taken from the flume side. Water content reflectometers (WCRs) were used to measure the temporal variation of moisture content during seepage process. Load cell and servo type water gauge were used to measure sediment and

total flow in the downstream end of the flume. pF meter with automatic pressure controller was used to determine the van Genuchten parameter of sand mixture used for the landslide dam.

Numerical simulations and flume experiments were performed to investigate the mechanism of landslide dam failure and resulting hydrograph due to overtopping and sudden sliding. Experimental conditions and parameters used for simulations in different cases are shown in Table 2. K and δ_d are the parameters of erosion and deposition velocity respectively. Following three cases are considered:

Table 2 Experimental conditions and parameters for simulation

Case	Q_{in} (cm³/sec)	Water content	Saturated hydraulic conductivity, K_s (m/sec)	K	δ_d
I	550	50%	0.00018	0.11	0.005
II	49	50%	0.00018	0.11	0.005
III	30.5	20%	0.00030	0.11	0.005

Case I: Overtopping (from full channel width)

Steady discharge of 550 cm³/sec was supplied from the upstream part of the flume. The model started simulation after the start of inflow. Overtopping occurred after the filling of the reservoir. Overtopped water proceeds downstream eroding the crest as well as the downstream slope of the dam body.

The simulated and experimental outflow hydrograph at 66cm downstream of the dam are
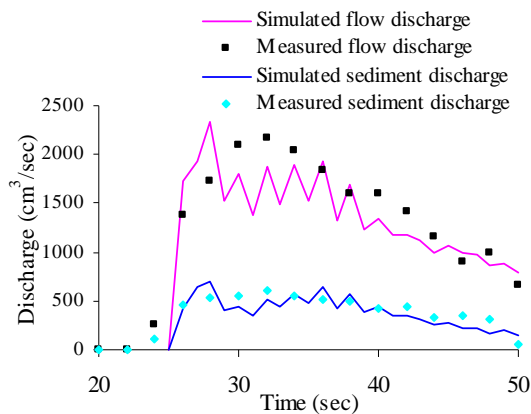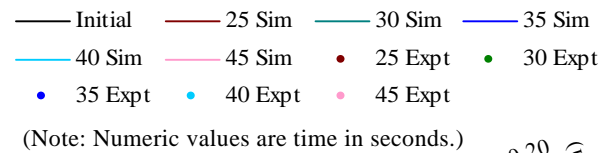

Fig. 3 Outflow hydrograph

Fig. 4 Comparison of dam surface erosion

represented in Fig. 3. Transformation of the dambody with time is shown in Fig. 4. The shape of the simulated surface of the dam body at each time steps are similar to observed. The simulated outflow hydrograph is not matching perfectly due to difference in time to overspill the reservoir and rate of dam surface erosion between simulation and experiment.

Case II: Overtopping and channel breach (from partial channel width)

Notch of the width 5cm and depth 0.5cm was incised at the crest and downstream face of the dam in the left side of the dam body so that the erosion of the surface of dam body can be observed from left side of the flume. Steady discharge of 49.0 cm³/sec was supplied from the upstream part of the flume, after the filling of the reservoir, it overflowed from the notch at the crest of the dam. The overtopping flow incised a channel on the slope of the dam and that channel increased its cross-sectional area with time caused by the erosion of released water. The simulated and experimental outflow hydrograph are represented in Fig. 5. Fig. 6 shows the comparison of the simulated and experimental shapes of dam surface at different time steps. In both experiment and simulation the channel incised almost vertically that may be due to rapid drawdown of reservoir and small inflow rate. The overflowing water depth was very small so the shear stress due to flowing water in the side wall of incised channel was also small and above the water level there was some apparent cohesion added by
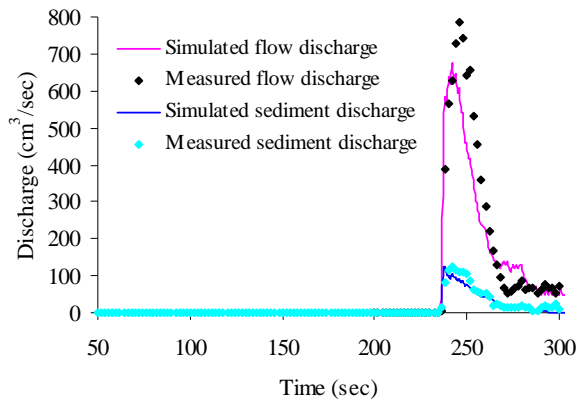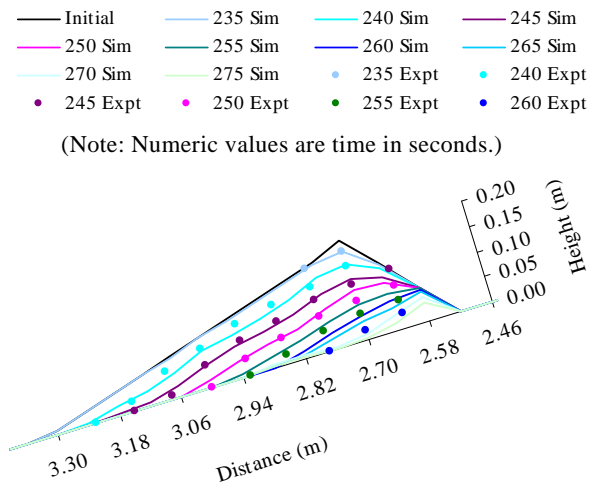
Fig. 5 Outflow hydrograph

Fig. 7 Comparison of simulated and experimental slip surface

(Note: Numeric values are time in seconds.)

Fig. 6 Comparison of dam surface erosion at incised channel

Fig. 8 Simulated and experimental results of water content profile for different WCRs

water content and adhesion so the side wall is very steep. Armouring effect is also negligible due to small particle size of the dam body.

Case III: Sudden sliding

Steady discharge of 30.5 cm³/sec was supplied from the upstream part of the flume. The sudden sliding of the dam body was observed at 447sec in the experiment whereas in the simulation it was observed at 410sec. The simulated time was slightly earlier than the experimentally observed time that may be due to the assumption of immobile air phase in unsaturated flow and variation of saturated hydraulic conductivity. Moreover, the effects of interslice forces are ignored in Janbu's simplified method. Increase in shear strength due to the negative pore-water pressures are not considered in the formulation of factor of safety. Fig. 7 shows the
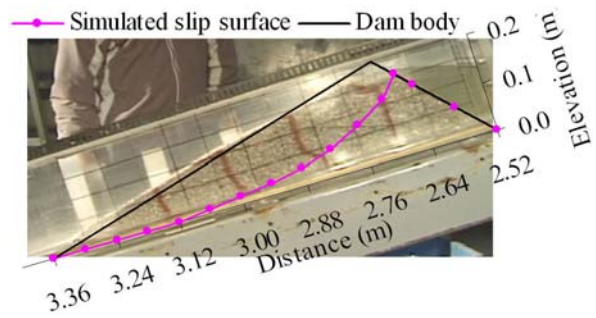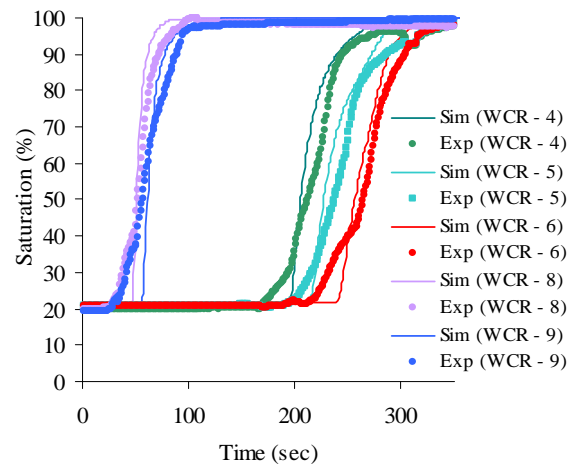
comparison of simulated and experimental slip surface. For the same experimental conditions, moisture content in the dam body was measured by using WCRs. Fig. 2 shows the locations of WCRs in the dam body. Fig. 8 shows the simulated and experimental results of moisture profile at WCR-4, WCR-5, WCR-6, WCR-8, and WCR-9 which are in good agreement. The geometry of predicted critical slip surface was also similar to that observed in the experiment.

Fig. 9 shows the simulated and experimental results of outflow hydrograph. There is some time lag between failure of dam and movement of the slipped soil mass but in the model, the time necessary for such a deformation is assumed as nil so the simulated peak is earlier than experimental peak. Peak discharge depends on the shape of the dam body assumed after sliding and parameters of erosion and deposition velocity.
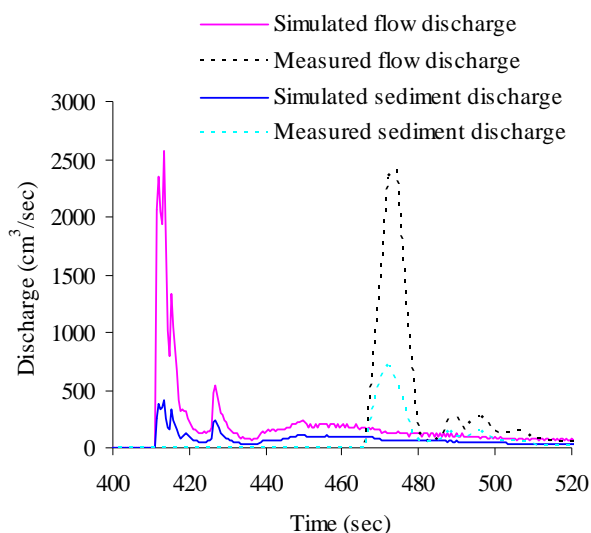
Fig. 9 Outflow hydrograph

The movement of moisture in the dam body measured by using WCRs, critical slip surface observed in the experiment and predicted outflow hydrograph are close to the result of numerical simulation.

5. Conclusions

An integrated model is developed for simulation of flood/debris flow hydrograph due to landslide dam failure by overtopping and sliding. The proposed model is tested for three different experimental cases of landslide dam failure due to overtopping and sliding and reasonably reproduced the resulting hydrograph. The numerical simulation and experimental results of movement of moisture in the dam body, predicted critical slip surface and time to failure of the dam body are also in good agreement. The predicted hydrograph can be used for flood disaster mitigation in the downstream. The model can be further extended to three-dimensions for the better representation of failure process of landslide dam.

References

Awal, R., Nakagawa, H., Baba, Y. and Sharma, R. H. (2007): Numerical and experimental study on landslide dam failure by sliding, Annual J. of Hydraulic Engineering, JSCE, Vol. 51, pp. 7-12.

Broich, K. (1988): Mathematical modeling of dambreak erosion caused by overtopping, Proceedings of the 2nd CADAM Workshop, Munich, October.

Costa, J. E. (1985): Floods from dam failures, U.S. Geological Survey, Open-File Rep. No. 85-560, Denver, 54.

Costa, J.E. and Schuster, R.L. (1988): The formation and failure of natural dams, Geological Society of America Bulletin 100, pp. 1054–106, 1988.

Davies,T.R., Manville, V., Kunz, M. and Donadini, L. (2007): Modeling Landslide Dambreak Flood Magnitudes: Case Study, Journal of Hydraulic Engineering, Vol. 133(7), pp. 713-720.

Fread, D. L. (1991): BREACH: an erosion model for earthen dam failures, U.S. National Weather Service, Office of Hydrology, Silver Spring, Maryland.

Mizuyama, T. (2006): Countermeasures to cope with landslide dams – prediction of the outburst discharge, Proc. Of 6th Japan-Taiwan Join Seminar on Natural Disaster Mitigation, (in CD ROM).

Morris, M. and Hassan, M. (2002): Breach formation through embankment dams & flood defense embankments: a state of the art review, Impact Project Workshop, H. R. Wallingford, UK.

Satofuka, Y., Yoshino, K., Mizuyama, T., Ogawa, K., Uchikawa, T. and Mori, T. (2007): Prediction of floods caused by landslide dam collapse, Annual J. of Hydraulic Engineering, JSCE, Vol.51, pp. 901-906 (in Japanese).

Swanson, F. J., Ouyagi, N. and Tominaga, M. (1986): Landslide dams in Japan, in Schuster, R. L., ed., Landslide Dams: Process, Risk and Mitigation: ASCE Geotechnical Special Publication, No. 3, pp. 131-145.

Tabata, S., Ikeshima, T., Inoue, K. and Mizuyama, T. (2001): Study on prediction of peak discharge in floods caused by landslide dam failure, Jour. of JSECE, Vol. 54, No. 4, pp. 73-76 (in Japanese).

Tabata, S., Mizuyama, T. and Inoue, K. (2002): Landslide dams and disasters, Kokon-shoin, pp. 205.

Takahashi T. and Kuang, S. F. (1988): Hydrograph prediction of debris flow due to failure of landslide dam, Annuals, Disas. Prev. Res. Inst., Kyto Univ., No. 31, B-2, pp. 601-615.

Takahashi T. and Nakagawa, H. (1994):

Flood/debris flow hydrograph due to collapse of a natural dam by overtopping, Journal of Hydroscience and Hydraulic Engineering, JSCE, Vol. 12, No. 2, pp. 41-49.

van Genuchten, M. Th. (1980): A closed-form equation for predicting the hydraulic conductivity of unsaturated soils, Soil Sci. Soc. Am. J., Vol. 44, pp. 892-898.

Walder, J. S. and O'Connor, J. E. (1997): Methods for predicting peak discharge of floods caused by failure of natural and constructed earthen dams, Water Resources Research, Vol. 33, No. 10, pp. 2337-2348.

Yamagami, T. and Ueta, Y. (1986): Noncircular slip surface analysis of the stability of slopes: An application of dynamic programming to the Janbu method, Journal of Japan Landslide Society, Vol. 22, No. 4, pp. 8-16.

天然ダムの越流及びすべり破壊に起因した洪水/土石流ハイドログラフの予測

Ripendra AWAL*・中川一・川池健司・馬場康之・張浩

*京都大学大学院工学研究科

要　旨

　本研究では，（ⅰ）浸透流解析モデル，（ⅱ）斜面安定モデル，（ⅲ）堤体表面侵食モデル，の３つのモデルを組み合わせることにより，天然ダムの越流及びすべり破壊に起因した洪水/土石流ハイドログラフの予測に関する統合的なモデルを開発した。統合的なモデルの主な特長は，ある初期条件及び境界条件下での天然ダム破壊が越流とすべりのどちらに起因する破壊なのかがわかることである。越流及びすべりに起因する天然ダムの破壊実験を３ケース行い提案したモデルの妥当性を検証した。その結果提案したモデルは実験から得た洪水流及び土石流ハイドログラフの結果を適切に再現することが確認された。

キーワード：天然ダム，斜面安定，浸透流，越流，洪水/土石流ハイドログラフ